

Observing *Zitterbewegung* with Ultracold Atoms

J. Y. Vaishnav and Charles W. Clark

Joint Quantum Institute, National Institute of Standards and Technology, Gaithersburg, Maryland 20899, USA
(Received 21 December 2007; published 16 April 2008)

We propose an optical lattice scheme which would permit the experimental observation of *Zitterbewegung* (ZB) with ultracold, neutral atoms. A four-level tripod variant of the setup for stimulated Raman adiabatic passage (STIRAP) has previously been proposed for generating non-Abelian gauge fields. Dirac-like Hamiltonians, which exhibit ZB, are simple examples of such non-Abelian gauge fields; we show how a variety of them can arise, and how ZB can be observed, in a tripod system. We predict that the ZB should occur at experimentally accessible frequencies and amplitudes.

DOI: 10.1103/PhysRevLett.100.153002

PACS numbers: 37.10.Vz, 37.10.Jk, 71.70.Ej

A driving force behind the study of ultracold atoms is their potential use as highly tunable quantum simulators for physical systems, ranging from quantum phase transitions in solids [1] to black holes [2]. In particular, the high degree of control over length and time scales in cold atom experiments allows for the possibility of observing phenomena that are experimentally inaccessible in their original counterpart systems. In this Letter, we propose an experiment which simulates the relativistic phenomenon of *Zitterbewegung* (ZB), a jittering motion first encountered in the Dirac theory of the electron [3].

ZB oscillations cannot be directly observed for a Dirac electron; their amplitude is the Compton wavelength, $h/mc \approx 10^{-12}$ m, which defines the limit of electron localization. Indirect consequences of ZB can, however, be seen in the response of electrons to external fields [3]. Furthermore, the presence of ZB is not unique to Dirac electrons, but rather is a generic feature of spinor systems with linear dispersion relations. Trapped ions [4], graphene [5–7], and semiconductor quantum wires [8] have been proposed as candidate systems for direct observation of ZB.

We propose a scheme for observing ZB in ultracold neutral atoms in optical lattices. We begin with a four-level “tripod” variant of the usual setup for stimulated Raman adiabatic passage (STIRAP) [9]. We find that the Hamiltonian for atoms in an optical lattice tripod configuration is Dirac-like in the subspace of the tripod’s two degenerate dark states. Thus, an atom’s mean position should undergo ZB. The characteristic amplitude of ZB oscillations in our tripod scheme is the wavelength, λ , of the light that produces the optical lattice, vs the Compton wavelength of Dirac ZB. The lattice’s recoil velocity (a few cm/s) replaces the speed of light in the Dirac theory. Tripod ZB thus falls well within the range of experimental observation, with a characteristic frequency of MHz vs the THz predicted for condensed matter implementations [7,8].

We consider the 2D optical lattice configuration shown in Fig. 1(a) and treat it from the tripod STIRAP perspective of [9]. Reference [9] describes the general derivation of the effective Hamiltonian for atomic motion in tripod setups;

we summarize the results here. The Hamiltonian in the interaction picture is $H = -\hbar \sum_{i=1}^3 \Omega_i |0\rangle\langle i| + \text{H.c.}$ Defining $\Theta_i = \sqrt{\sum_{j=1}^i |\Omega_j|^2}$, the dressed states include two dark states degenerate at zero energy: $|D_1\rangle = \frac{1}{\Theta_2} \times (\Omega_2|1\rangle - \Omega_1|2\rangle)$ and $|D_2\rangle = \frac{1}{\Theta_3} (\Omega_1^* \Omega_3|1\rangle - \Omega_2^* \Omega_3|2\rangle - \Theta_2^2|3\rangle)$ (we have chosen an orthonormal basis). Suppose the atoms are now slowly moving in the field. The degeneracy causes the Born-Oppenheimer approximation to break, yielding an effective U(2) non-Abelian gauge field. The effective Hamiltonian in the 2×2 dark subspace is $H = \frac{1}{2m} (\vec{p} - \hat{\mathbf{A}})^2 + \hat{\Phi}$, where m is the atom’s mass, $\mathbf{A}_{i,j} = i\hbar \langle D_i | \vec{\nabla} | D_j \rangle$ is an effective vector potential, and $\hat{\Phi}$ is a scalar Born-Huang potential resulting from the coupling to the bright subspace (we refer the reader to [9] for details). We choose parameters Ω and $-1 \leq \epsilon \leq 1$ so that the Rabi frequencies indicated in Fig. 1(a) are given by

$$\Omega_1(\vec{r}) = \Omega \sqrt{1 - \epsilon^2} \cos k_0 z, \quad (1)$$

$$\Omega_2(\vec{r}) = -\Omega \sqrt{1 - \epsilon^2} \sin k_0 z, \quad (2)$$

$$\Omega_3(\vec{r}) = \epsilon \Omega e^{ik_0 y}, \quad (3)$$

where $k_0 = 2\pi/\lambda$. Related setups were proposed for observing spin relaxation effects [10] and negative refraction [11]. After some gauge transformations, the two dark states

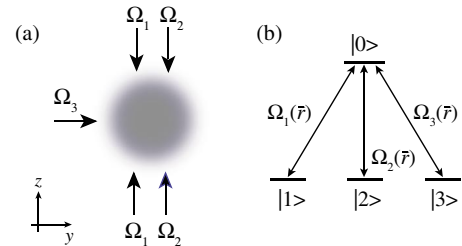


FIG. 1 (color online). (a) Schematic geometry of tripod laser beams yielding the Rabi frequencies of Eqs. (1)–(3). (b) Tripod STIRAP scheme with Rabi frequencies as defined in Eqs. (1)–(3).

TABLE I. By tuning ε and choosing different states to represent spin-up, the tripod setup can replicate a variety of Dirac-like Hamiltonians (see, e.g., [6]). Reference [13] proposes an alternate method of generating a graphenelike Hamiltonian.

Spin-up	ε	H	Analog
$ D_1\rangle$	ε_R	$H = \frac{p^2}{2m} + \alpha(p_y\sigma_z - p_z\sigma_y)$	Rashba
$\frac{1}{\sqrt{2}}(D_1\rangle + i D_2\rangle)$	ε_R	$H = \frac{p^2}{2m} + \alpha(p_y\sigma_y - p_z\sigma_z)$	Linear Dresselhaus
$\frac{1}{\sqrt{2}}(D_1\rangle + i D_2\rangle)$	$-\varepsilon_R$	$H = \frac{p^2}{2m} + \alpha(p_y\sigma_y + p_z\sigma_z)$	Graphene sheet, in vicinity of Dirac point

feel an effective vector potential

$$\hat{A}_y = \frac{\hbar k_0}{2}(1 - \varepsilon^2)\sigma_z, \quad (4)$$

$$\hat{A}_z = -\varepsilon\hbar k_0\sigma_y, \quad (5)$$

and an effective scalar potential $\hat{\Phi} = V_0\sigma_z$, where $V_0 = \hbar^2 k_0^2/(2m)(1 - \varepsilon^2)$. In general, $[\hat{A}_y, \hat{A}_z] \neq 0$, so the effective gauge field is non-Abelian.

We can write the full Hamiltonian in the dark subspace as

$$H = \frac{p^2}{2m} - \frac{\hbar k_0}{2m}[(1 - \varepsilon^2)p_y\sigma_z - 2\varepsilon p_z\sigma_y] + V_0\sigma_z. \quad (6)$$

The middle term in Eq. (6) is Dirac-like, with the lattice recoil velocity $\hbar k_0/2m$ taking the place of the speed of light. Thinking of $|D_{1(2)}\rangle$ as “spin-up (-down)”, the Hamiltonian of Eq. (6) is effectively a spin-orbit coupling, in the presence of a homogeneous magnetic field along the z direction. In fact, letting $\alpha = \hbar k_0\varepsilon/m$, and choosing $\varepsilon_R = \sqrt{2} - 1 = \varepsilon$, we have $H = \frac{p^2}{2m} + \alpha(p_y\sigma_z - p_z\sigma_y) + V_0\sigma_z$ —the Hamiltonian for a 2D electron gas in the y - z plane, with Rashba spin-orbit coupling, and subject to a homogeneous magnetic field along the z axis. Reference [12] proposes an alternate scheme for generating spin-orbit coupling with ultracold atoms.

We can remove the scalar potential by applying a state-dependent external potential to the system. Denoting the potential felt by $|i\rangle$ as $V_i(\vec{r})$, choosing $V_1(\vec{r}) = V_2(\vec{r}) = V(\vec{r})$, and $V_3(\vec{r}) = V(\vec{r}) + V_0(1 + \varepsilon^2)/(1 - \varepsilon^2)$ subjects the dark states to an additional potential $\hat{V} = V(\vec{r}) \otimes \mathbf{I} - \hat{\Phi}$. If the scalar potential is thus removed from Eq. (6), the resulting Hamiltonian is extremely versatile, for two reasons: (i) ε is tunable and (ii) the dark states form a degenerate subspace, for which any basis is equivalent. In fact, depending on the direction we call spin-up, this Hamiltonian can be viewed as a variety of Dirac-like Hamiltonians (see Table I).

The eigenstates of the system are spinors $e^{ik_y y} e^{ik_z z} \otimes |i; \vec{k}\rangle$ with $i = a, b$ and \vec{k} the atom’s momentum; the $|i; \vec{k}\rangle$ are defined below. The dispersion relation of the Hamiltonian in Eq. (6) is

$$E_{\pm}(k_y, k_z) = \frac{\hbar^2 k^2}{2m} \pm \frac{\hbar^2 k_0}{m} \sqrt{(1 - \varepsilon^2)^2(k_y - k_0)^2 + (2\varepsilon)^2 k_z^2}. \quad (7)$$

The energy surfaces in Eq. (7) have a conical intersection

at $(k_y, k_z) = (k_0, 0)$ (see Fig. 2). Defining

$$\tan \xi(\vec{k}) = 2\varepsilon k_z / [(1 - \varepsilon^2)(k_y - k_0)], \quad (8)$$

we designate the eigenfunctions by $|a; \vec{k}\rangle = [i \sin \frac{\xi(\vec{k})}{2}, \cos \frac{\xi(\vec{k})}{2}]^T$, $|b; \vec{k}\rangle = [i \cos \frac{\xi(\vec{k})}{2}, -\sin \frac{\xi(\vec{k})}{2}]^T$. As the physical signature of a conical intersection is a Berry phase, the eigenfunctions are multivalued for a particular (k_y, k_z) . The momentum-space Berry phase is much like the one encountered in graphene, which gives rise to phenomena like the half-integer quantum Hall effect [14]. We now examine the role that the Berry phase plays in generating ZB.

Consider the time evolution of a Gaussian wave packet prepared in a superposition of dark states. In the non-Abelian case ($0 < \varepsilon < 1$), the eigenvectors have an associated Berry phase, and are both \vec{k} dependent and multivalued. However, the initial spin state must be single valued, forcing its expansion coefficients to be \vec{k} dependent (and also multivalued). The presence of the Berry phase thus translates into a \vec{k} dependence of $\xi(\vec{k})$ in Eq. (8); we later show that it is this nonvanishing $\vec{\nabla}_{\vec{k}} \xi(\vec{k})$ that gives rise, directly, to ZB.

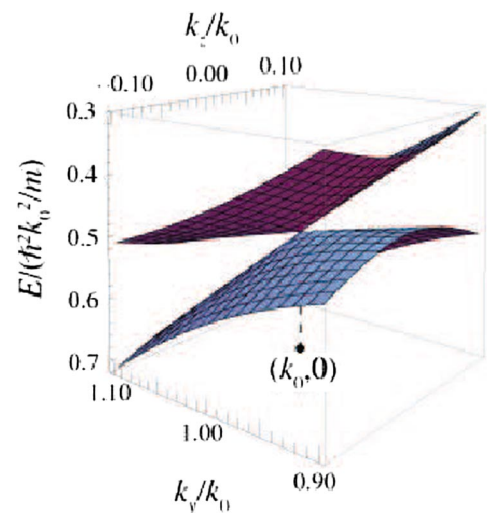


FIG. 2 (color online). Energy surfaces in momentum space for ^{85}Rb with $k_0 = 2\pi/820 \text{ nm}^{-1}$ and $\varepsilon = \varepsilon_R$. A conical intersection occurs at $(k_y, k_z) = (k_0, 0)$; a circuit of this conical intersection in \vec{k} space gives a Berry phase.

Considering an initial wave packet

$$\psi(\vec{r}; 0) = \frac{1}{\sqrt{2}} \int d\vec{k} g(\vec{k}; 0) e^{i\vec{k}\cdot\vec{r}} \begin{pmatrix} 1 \\ 1 \end{pmatrix}, \quad (9)$$

it is straightforward to show that its time evolution is

$$\begin{aligned} \psi(\vec{r}; t) &= \frac{1}{\sqrt{2}} \int d\vec{k} g(\vec{k}; 0) e^{i\vec{k}\cdot\vec{r}} e^{-iE_0(\vec{k})t/\hbar} \\ &\times \left\{ \cos[\omega(\vec{k})t] \begin{pmatrix} 1 \\ 1 \end{pmatrix} - i e^{-i\xi(\vec{k})} \sin[\omega(\vec{k})t] \begin{pmatrix} 1 \\ -1 \end{pmatrix} \right\}, \end{aligned} \quad (10)$$

where $\omega(\vec{k}) = \frac{1}{2\hbar} (E_+(\vec{k}) - E_-(\vec{k}))$.

ZB, in the Dirac equation, is an oscillation of the average position $\langle \vec{r}(t) \rangle$. The usual method of understanding the Dirac equation, and related equations is to derive equations of motion for the Heisenberg operators, and show that they oscillate in time [6–8]. We instead work in the Schrödinger picture, which makes explicit the connection to Berry phase. As $[H, p] = 0$, it is convenient to work in the momentum basis, and calculate

$$\langle \vec{r}(t) \rangle = i \int d\vec{k} \vec{\phi}^\dagger(\vec{k}; t) \cdot \vec{\nabla}_{\vec{k}} \vec{\phi}(\vec{k}; t),$$

where $\vec{\psi}(\vec{r}; t) = \int d\vec{k} \vec{\phi}(\vec{k}; t) e^{i\vec{k}\cdot\vec{r}} / (2\pi)$ is the spinor wave function. After some algebra, we find

$$\begin{aligned} \langle \vec{r}(t) \rangle &= \langle \vec{r}(0) \rangle + \frac{\hbar \langle \vec{k}(0) \rangle}{m} t + \frac{1}{2} \int d\vec{k} |g(\vec{k}; 0)|^2 (\vec{\nabla}_{\vec{k}} \xi(\vec{k})) \\ &\times [1 - \cos 2\omega(\vec{k})t], \end{aligned}$$

where the final term, which oscillates in time, is ZB. The amplitude of the oscillation is proportional to $\vec{\nabla}_{\vec{k}} \xi(\vec{k})$. We had previously shown that the \vec{k} dependence of $\xi(\vec{k})$ occurs as a direct consequence of the eigenfunctions being multi-valued. The Schrödinger picture thus illuminates what is not evident in the Heisenberg representation—that the ZB here can be viewed as a measurable consequence of the momentum-space Berry phase.

We now propose an experimental demonstration of ZB using ultracold atoms. Suppose an ensemble of atoms is prepared in the vibrational ground state of a harmonic trap. The atom is initially prepared in a superposition of dark states, after which the trap is switched off to allow ballistic expansion. The initial wave packet can be approximated by a Gaussian function $g(\vec{k}; 0) = \frac{d}{\sqrt{\pi}} e^{-(1/2)(\vec{k}-\vec{k}^{(i)})^2 d^2}$, where d is the oscillator length of the trap, and $\vec{k}^{(i)}$ is a momentum boost (which is zero for the case of a stationary trap). For this wave packet, the expectation values of y and z oscillate as

$$\begin{aligned} \begin{pmatrix} \langle y(t) \rangle \\ \langle z(t) \rangle \end{pmatrix} &= \frac{\hbar \vec{k}^{(i)}}{m} t + \frac{d}{2\pi} \int d\vec{k} e^{-(\vec{k}-\vec{k}^{(i)})^2 d^2} \frac{1}{\vec{k}^2} \\ &\times [1 - \cos 2\omega(\vec{k})t] \begin{pmatrix} (\varepsilon^2 - 1)\vec{k}_z \\ 2\varepsilon\vec{k}_y \end{pmatrix}, \end{aligned} \quad (11)$$

where we have defined $\vec{k}_y = (1 - \varepsilon^2)k_y$, $\vec{k}_z = 2\varepsilon k_z$, and $\vec{k} = \sqrt{\vec{k}_y^2 + \vec{k}_z^2}$. Equation (11) shows that the ZB vanishes in the Abelian cases, $\varepsilon = 0$ or $\varepsilon = 1$.

It is useful to consider the limit $d \rightarrow \infty$, where $g(\vec{k}; 0) \rightarrow \delta(\vec{k} - \vec{k}^{(i)})$; i.e., the initial wave packet approaches a plane wave. The integrals in Eqs. (11) become trivial, and we find that

$$\begin{aligned} \begin{pmatrix} \langle y(t) \rangle \\ \langle z(t) \rangle \end{pmatrix} &= \frac{\hbar \vec{k}^{(i)}}{m} t + \frac{1}{2(\vec{k}^{(i)})^2} [1 - \cos 2\omega(\vec{k}^{(i)})t] \\ &\times \begin{pmatrix} (\varepsilon^2 - 1)\vec{k}_z^{(i)} \\ 2\varepsilon\vec{k}_y^{(i)} \end{pmatrix}. \end{aligned}$$

In the opposite limit, $d \rightarrow 0$, the ZB vanishes, and for intermediate values the energy spread causes damping, as can be shown analytically for bilayer graphene [7].

Because of the induced Born-Huang field, ZB will occur in this system even if the wave packet has an initial zero group velocity (in contrast to the condensed matter counterparts [6–8]). For ^{87}Rb atoms with $k_0 = (2\pi/820) \text{ nm}^{-1}$, and a Gaussian with $\vec{k}^{(i)} = \vec{0}$ and width $k_0 d = 16.2$, corresponding to the ground state of a trap with trap frequency 112 Hz, we find that a pronounced oscillation would occur in the z direction before damping out (Fig. 3). A typical time scale of the ZB here would be μs rather than the fs predicted in, e.g., graphene and related systems [7]. The damping time of the ZB is inversely proportional to the momentum spread of the initial wave packet.

We have shown that the mean position of the atom oscillates sinusoidally. However, ZB can also be viewed in terms of state-resolved spatial dynamics. For the Gaussian initial wave packet, it is not difficult to show that as the center of mass of the cloud is oscillating in the z

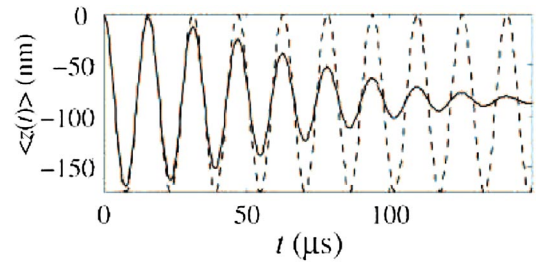


FIG. 3 (color online). ZB for an atom with zero momentum spread (dashed), and for a momentum spread corresponding to the velocity spread of a cloud initially in a trap of frequency 112 Hz (solid). ZB oscillations for finite momentum spread damp out over time, but persist over several periods.

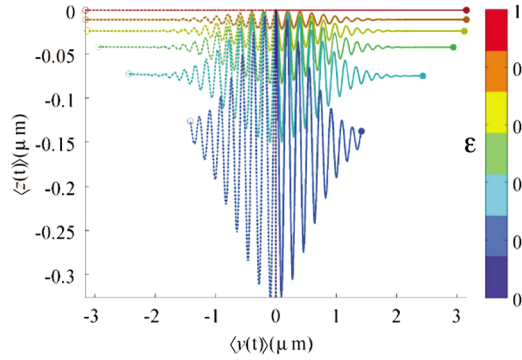


FIG. 4 (color online). Spin separation and ZB for $\varepsilon = 0(0.2)1$, as indicated on the right color bar. For each value of ε the dashed trajectory corresponds to the atom's mean position in spin-up, while the solid trajectory corresponds to the mean position of the atom in spin-down; open and closed circles indicate the respective ends of these trajectories. In the Abelian cases, $\varepsilon = 0$ and 1, the trajectories are straight lines; the trajectory for $\varepsilon = 0$ is the vertical line $y = 0$.

direction, in the y direction, the wave packet separates by spin, such that $\langle y_{1,2}(t) \rangle = \pm \hbar k_0 t / m$ (see Fig. 4). This spin separation, which coexists with the ZB, is a manifestation of the atomic spin Hall effect proposed in a different setup [15]; a related effect occurs in velocity-selective coherent population trapping [16].

Figure 5 shows the dynamics of the spin-up component of the wave packet in a representative non-Abelian case. The effective magnetic field deflects spin-up and spin-down in opposite directions. As the two wave packets separate, the coupling between the components results in oscillating “tails” on the wave packets, giving rise to ZB. The ZB decays as the wave packets separate and cease to interfere.

We note that the Hamiltonian for N particles in the non-Abelian gauge field, interacting via two-body interactions, separates in center of mass and relative coordinates, \vec{R} and $\vec{\rho}$ respectively. The Hamiltonian is then $\hat{H} = \hat{H}_{\text{CM}} + \hat{H}_{\vec{\rho}}$, where $\hat{H}_{\vec{\rho}}$ is a function only of the relative coordinates $\vec{\rho}$, and

$$\hat{H}_{\text{CM}} = \frac{1}{2mN} \vec{P}^2 - \frac{\hbar k_0}{2m} \sum_i [(1 - \varepsilon^2)(P_y + \hbar k_0) \Sigma_z - 2\varepsilon P_z \Sigma_y],$$

where \vec{P} is the center-of-mass momentum and $\vec{\Sigma} = \sum_i \vec{\sigma}^{(i)}$ is the total spin. The Hamiltonian for the center of mass is thus again of a single-particle Dirac form (with a higher spin), and in a dilute cloud of N particles with two-body interactions, the center of mass of the cloud undergoes ZB.

In this Letter, we have examined the dynamics of an atom in a tripod level scheme on an optical lattice; this common experimental setup gives rise to a non-Abelian gauge field which is isomorphic to the spin-orbit interaction in 2D electron gases. The idea of atomtronics, or engineering atomic versions of semiconductor devices,

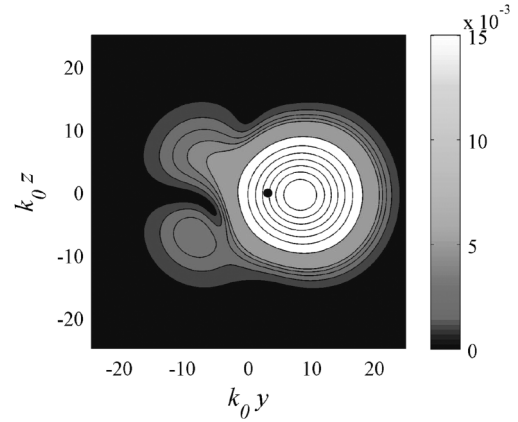


FIG. 5. Time-evolved probability distribution in spin-up for an initial Gaussian wave packet ($\varepsilon = \varepsilon_R$, $k_0 d = 5$, $\hbar k_0^2 t / m = 10$). As seen in Fig. 4, the wave packet separates by internal state as it jitters; the black dot indicates the mean position, which has drifted to the right. The mixing between internal states gives rise to tails on the wave packet, resulting in ZB. The ZB damps as the internal states separate.

has generated interest [17]; the prospect of engineering artificial spin-orbit couplings suggests the possibility of atomic “spintronics”, for example, engineering atomic counterparts of devices such as the Datta-Das transistor [18], which have yet to be successfully realized with electrons. The tripod system here exhibits atomic ZB at MHz frequencies, vs the THz frequencies offered by recently discussed condensed matter systems [7,8]. We believe it is a promising candidate for the experimental observation of ZB.

-
- [1] D. Jaksch *et al.*, Phys. Rev. Lett. **81**, 3108 (1998).
 - [2] L. Garay *et al.*, Phys. Rev. Lett. **85**, 4643 (2000).
 - [3] K. Huang, Am. J. Phys. **20**, 479 (1952).
 - [4] L. Lamata *et al.*, Phys. Rev. Lett. **98** 253005 (2007).
 - [5] M. Katsnelson, Eur. Phys. J. B **57**, 225 (2007).
 - [6] J. Cserti and G. Dávid, Phys. Rev. B **74**, 172305 (2006).
 - [7] T.M. Rusin and W. Zawadzki, Phys. Rev. B **76**, 195439 (2007).
 - [8] J. Schliemann, D. Loss, and R. Westervelt, Phys. Rev. Lett. **94**, 206801 (2005).
 - [9] J. Ruseckas *et al.*, Phys. Rev. Lett. **95**, 010404 (2005).
 - [10] T.D. Stanescu, C. Zhang, and V. Galitski, Phys. Rev. Lett. **99**, 110403 (2007).
 - [11] G. Juzeliūnas, J. Ruseckas *et al.*, Phys. Rev. A **77**, 011802 (2008).
 - [12] A.M. Dudarev *et al.*, Phys. Rev. Lett. **92**, 153005 (2004).
 - [13] S.-L. Zhu, B. Wang, and L.-M. Duan, Phys. Rev. Lett. **98**, 260402 (2007).
 - [14] Y. Zhang *et al.*, Nature (London) **438**, 201 (2005).
 - [15] S.-L. Zhu *et al.*, Phys. Rev. Lett. **97**, 240401 (2006).
 - [16] A. Aspect *et al.*, J. Opt. Soc. Am. B **6**, 6 (1989).
 - [17] A. Ruschhaupt and J. Muga, Phys. Rev. A **70**, 061604 (2004).
 - [18] S. Datta and B. Das, Appl. Phys. Lett. **56**, 665 (1990).